

rate parts  $x$  and  $y$  of the graphs a tendency to a concerted variation of readings, which may possibly be linked with container's rotation, i.e., the growth of signals over one channel accompanied by a decrease of signals over the other. However, it should be noted that cases of monotonous variation of the continuity of signals are not scarce even on the pre-lunar part of the trajectory (Fig. 2). As a whole, readings along channels  $x$  and  $y$  are not in agreement, although curves similar to those of Fig. 1, obtained in the small terrestrial field, may not be expected here due to the short period of measurement in the immediate vicinity of the moon.

The experimental data must satisfy still another condition: the values of the total field's vector, computed from the data of components  $x$ ,  $y$ ,  $z$  of the field, must decrease according to the inverse cube law of distance from the center of the moon. After the aforementioned estimation of signal reliability along separate channels of the magnetometer, the computation of the values of the total vector from the data of separate channels becomes a formal operation. This must be borne in mind when examining graphs of Fig. 3. In the upper graphs the values of the total vector and the theoretical curves linked with separate readings (indicated by small circles) are plotted, assuming that they are more reliable. As may be seen from the graphs, the aggregate of the computed field values does not satisfy either of the theoretical curves brought forth sufficiently.

Therefore, as a result of the analysis of experimental materials at fractional distances of the lunar radius from the surface of the moon, we discovered no reliable indications of the presence of an external magnetic field on the moon.

Using the aggregate of experimental data obtained at fractional distances of the radius from the surface of the moon, we may determine the magnitude of uncertainty of our knowledge of the moon's field. For that purpose we used a theoretical curve closest to experimental values. Thus determined, the effective magnetic moment of the moon cannot, in any case, be greater than  $6 \cdot 10^{21}$  CGSM (cm gr/sec magnetic units), which constitutes about 1/10000 of the earth's magnetic moment.

The result obtained, which attests to the absence of a noticeable dipole-type field near the moon, agrees well with the results of measurement of cosmic radiation near the moon.<sup>1</sup> It is well known that no cosmic radiation belts were detected near the moon.

The first magnetic field measurements near the moon, completed during the flight of the second Soviet cosmic rocket, made it possible to establish that the moon does not have a notable magnetic field. Its dipole magnetic moment can only be less than 1/10,000 of the earth's magnetic moment. This result gives evidence in favor of the contemporary hypothesis of the origin of the earth's magnetic field. Aside from making the lower boundaries more precise, subsequent experiments may provide information as to whether the moon had a magnetic field in the past and on the genesis of its surface and its cosmogonic history.

—Submitted December 13, 1960

<sup>1</sup> Vernov, S. I., Chudakov, A. E., Vakulov, I. V., Logachev, Yu. I., and Nikolayev, A. G., "Radiation measurements during the flight of the second cosmic rocket," *Iskusstvennye Sputniki Zemli (Artificial Earth Satellites)* (1960), no. 5.

FEBRUARY 1963

AIAA JOURNAL

VOL. 1, NO. 2

## Outer Radiation Belt of the Earth at 320 km Altitude

S. N. VERNOV, I. A. SAVENKO, P. I. SHAVRIN, V. I. NESTEROV, and N. F. PISARENKO

THE existence of the earth's outer radiation belt, clearly limited to the high latitude region, was shown as a result of investigations completed on the second and third Soviet artificial earth satellites (1).<sup>1</sup>

The scintillation and gas-discharge counters aboard the second Soviet spaceship permitted a detailed investigation of the outer radiation belt near the earth and a determination of its boundaries in relation to the longitude. The second spaceship's orbit was nearly circular, and it was situated within an altitude range of 306 to 339 km (2).

An automatic memory device aboard the spaceship provided the means for a continuous flow of information on radiation intensity at indicated heights within the  $\pm 65^\circ$  latitude range and along the whole of the earth. The output from the scintillation and gas-discharge counters was read into the memory every three minutes.

The scintillation counter consisted of a cylinder-shaped NaI(Tl) crystal (height—14 mm, diameter—30 mm) and an FEU-16 photomultiplier, and the energy threshold of the counter's channel was 25 kev. The gas-discharge counter was of the STS-5 type (halogen-quenched counter).

Translated from *Iskusstvennye Sputniki Zemli (Artificial Earth Satellites)* (Publishing House of the Academy of Sciences USSR, 1961), no. 10, pp. 34-39. Translated by Andre L. Brichant for NASA Headquarters.

<sup>1</sup> Numbers in parentheses indicate References at end of paper.

The distribution of radiation intensity around the earth, as recorded by the scintillation counter, is shown in Fig. 1. The numbers indicate the intensity in  $\text{pulse} \cdot \text{cm}^{-2} \cdot \text{sec}^{-1}$ , assuming that the radiation incident on the crystal was isotropic. It follows from Fig. 1 that during the passing of the spaceship from the Equator to  $\pm 40$ – $50^\circ$  latitudes, the intensity registered by the scintillation counter gradually increased from 3–5  $\text{pulse} \cdot \text{cm}^{-2} \cdot \text{sec}^{-1}$  to about 8–10, because of latitude effect of cosmic rays, and then in most cases sharply increased to 20–600  $\text{pulse} \cdot \text{cm}^{-2} \cdot \text{sec}^{-1}$  in the region of  $50^\circ$  to  $65^\circ$  of geographic latitudes, and it remained only at times at the 13–15  $\text{cm}^{-2} \cdot \text{sec}^{-1}$ . The regions of increased intensity that cannot be explained by latitude effect of cosmic rays are crosshatched and bounded by a dash-dotted line.

It is quite natural to assume that this sharp increase in the rate of the scintillation counter is due to particles from the earth's radiation belts. To demonstrate that assumption, we analyzed the connection between the zones of increased intensity in the Northern and Southern hemispheres, and we also examined the relationship between the limits of the increased intensity with the characteristics of the earth's magnetic field. We finally established the content and appraised the energy of the registered radiation.

In Fig. 2 circles indicate the points at which the counting rate of the scintillator corresponded to intensities greater than 30  $\text{pulse} \cdot \text{cm}^{-2} \cdot \text{sec}^{-1}$ . The following geographic zones of in-

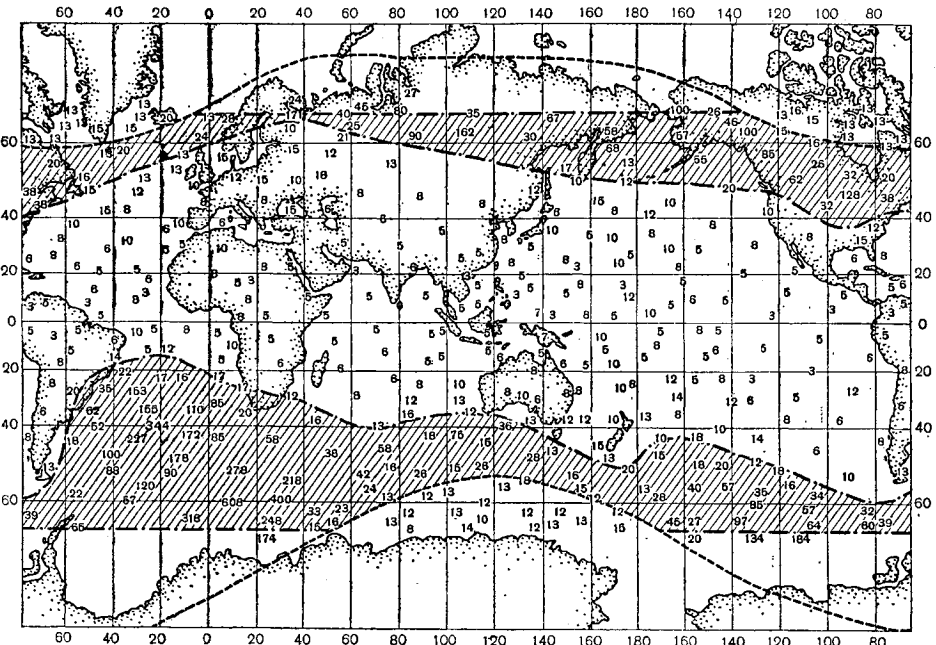


Fig. 1 Intensity registered by the scintillation counter ( $\text{pulse} \cdot \text{cm}^{-2} \cdot \text{sec}^{-1}$ ), at 320 km above various points of the globe. The lines of maximum aurora recurrence are indicated by the dashed line. The region in which the increased intensity cannot be explained by latitude effect of cosmic rays is crosshatched

creased intensity may be outlined conventionally: 1) Siberia, 2) North America, 3) Southern Indian Ocean, 4) South Pacific, and 5) the southern part of the Atlantic Ocean.

In order to establish a connection between the zones of the Northern and Southern hemispheres, we located the conjugate points, i.e., the ends of the lines of force of the geomagnetic field, whose beginning coincides with the points of increased radiation. The conjugate points calculated according to magnetic measurement data at the earth's surface (3), are represented in Fig. 2 by crosses, some of which are connected with the initial points by dashed lines. It follows from Fig. 2 that the first zone (Siberia) is conjugate to the third (South Indian Ocean), whereas the second (North America) is conjugate to the fourth (South Pacific).

On the other hand, the boundary between these two zones (Alaska-Chukotka) is conjugate to the area of the Pacific (New Zealand) where the intensity registered by the scintillation counter does not exceed 30  $\text{pulse} \cdot \text{cm}^{-2} \cdot \text{sec}^{-1}$ . Similarly, the black circles are absent in the North Atlantic, conjugate to the western edge of the third zone. However, analysis of experimental data has shown that an increased radiation in-

tensity was observed also in the regions of the North Atlantic and New Zealand which could not be explained by latitude effect of cosmic rays. Points where the intensity remained within the 15 to 30  $\text{pulse} \cdot \text{cm}^{-2} \cdot \text{sec}^{-1}$  range are represented in Fig. 2 by white circles. The radiation intensity in these places is lower than in conjugate regions because the greater value of the magnetic field strength leads to an increase of mirror point altitude. (For example, in the Alaska region  $B = 0.56$  oe and in the conjugate region of New Zealand  $B = 0.68$  oe.)

Therefore, the zones of increased radiation in the Northern hemisphere are linked with the zones of the Southern hemisphere by lines of force of the geomagnetic field, and the position of the belt with increased radiation at 320 km altitude is determined by that field.

The fifth zone of increased radiation linked with the South Atlantic anomaly of the earth's magnetic field is unique. This zone will be examined in another paper and therefore will be disregarded here.

The boundary of increased intensity belt at 300 km altitude at the side of higher latitudes adjoins in a series of spots the

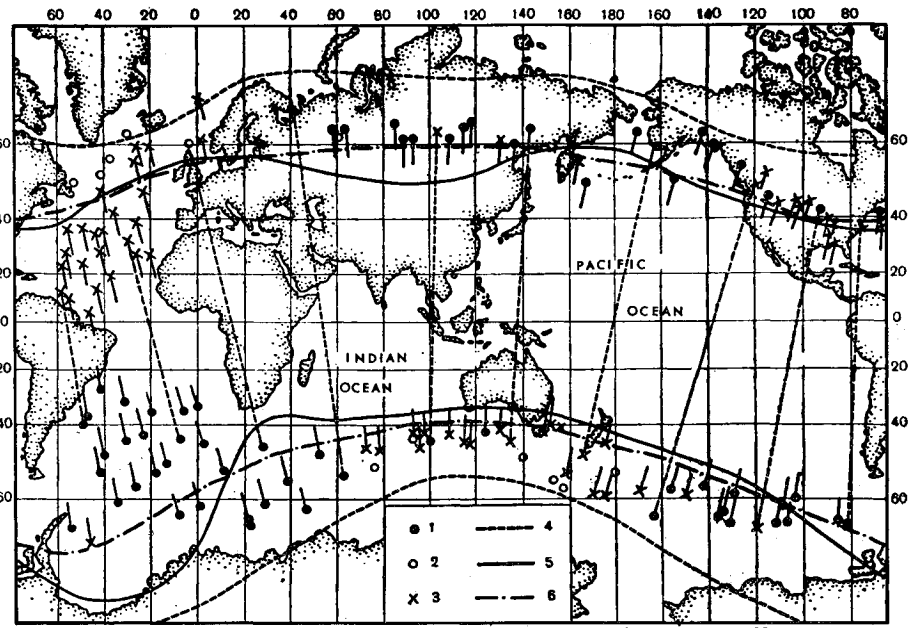


Fig. 2. Mutual distribution of zones of increased intensity in the Northern and Southern hemispheres, according to measurements made at 320-km altitude. 1) Points at which the counting rate of the scintillator exceeds  $30 \text{ cm}^{-2} \text{ sec}^{-1}$ ; 2) points at which the counting rate is 15 to  $30 \text{ cm}^{-2} \text{ sec}^{-1}$ ; 3) magnetic-conjugated points; 4) lines of maximum occurrence of auroras; 5) isoclines; 6) mirror point trajectories calculated from adiabatic integral invariants for particles trapped in the earth's magnetic field.

Tables 1 and 2 Counter readings at flight through the zone of increased intensity

Table 1 Northern hemisphere

$N_{sc}^a$ , pulse·cm $^{-2}$ ·sec $^{-1}$	$E^b$ , 10 $^7$ ev· cm $^{-2}$ ·sec $^{-1}$	Intensity according to STS-5 data, $N_G$ , pulse· cm $^{-2}$ ·sec $^{-1}$	$N_{sc} - N_{sc,beg}$ , pulse· cm $^{-2}$ ·sec $^{-1}$	$E - E_{beg}$ , pulse· cm $^{-2}$ ·sec $^{-1}$	$N_G - N_{G,beg}$ , pulse· cm $^{-2}$ ·sec $^{-1}$	$\frac{E - E_{beg}}{N_{sc} - N_{sc,beg}}$ , kev/pulse	$\frac{\epsilon_G}{\epsilon_{sc}} \cdot 10^3$
162	4.4	3.6	148	0.9	0.3	61	2.0
157	4.4	4.0	143	0.9	0.8	63	5.6
128	3.7	3.3	114	0.3	0.1	26	0.8
100	4.8	3.5	86	1.4	0.2	163	2.3
90	3.1	3.5	76	-0.3	0.2	-40	2.6
85	5.1	3.6	71	1.6	0.4	264	5.7
80	4.8	3.5	66	1.4	0.2	313	3.0

Table 2 Southern hemisphere

400	9.8	4.6	388	6.5	1.5	168	3.8
248	10.1	4.1	236	6.8	1.0	288	4.2
218	4.8	3.6	206	1.6	0.5	78	2.4
174	9.0	3.5	162	5.7	0.4	352	2.5
75	3.5	3.6	63	0.3	0.5	47	8.0

<sup>a</sup> Intensity according to data of the scintillation counter.

<sup>b</sup> Energy flux liberated in the crystal.

line of maximum aurora recurrence indicated in Fig. 1 by a dashed line (3). At the side of low latitudes, the belt's boundary coincides more or less with the isocline  $\delta = 70^\circ$  in the Northern hemisphere and with the isocline  $\delta = 66^\circ$  in the Southern hemisphere (solid lines in Fig. 2), which corresponds to magnetic latitudes  $\varphi = 54^\circ$  and  $\varphi = -48^\circ$ . The magnetic latitudes are determined from the correlation

$$\tan\varphi = \frac{1}{2}\tan\delta$$

where  $\delta$  is the magnetic angle of inclination.

The position of the belt of increased intensity coincides well with the mirror point trace calculated by using adiabatic integral invariants for particles trapped in the magnetic field of the earth (4). Dashed-dotted lines indicate the line of mirror points in Fig. 2, and, at the same time, the height of the mirror point was arbitrarily chosen to be about 1500 km at  $+120^\circ$  longitude.

In order to determine the composition and energy of the radiation recorded in the zones of increased intensity, we shall compare the readings of the scintillator and Geiger counters (Tables 1 and 2).

Table 1 gives a series of counter readings at flight through the zone of increased intensity in the Northern hemisphere. The readings that are ascribable to cosmic rays in the given latitudes (columns 4-6) are subtracted. In order to determine the cosmic ray background, advantage was taken of the fact that in the region adjacent to the Northern magnetic pole, namely in the  $-30$  to  $-120^\circ$  longitude range, the increased intensity belt lies at latitudes below  $+60^\circ$  (Fig. 1). During the flight through the region to the north of increased intensity belt, 16 counter reading determinations were made, and the following values of the background due to cosmic rays were obtained:

$$N_{sc,beg} = (13.9 \pm 0.3) \text{ pulse} \cdot \text{cm}^{-2} \cdot \text{sec}^{-1}$$

$$E_{beg} = (3.46 \pm 0.15) 10^7 \text{ ev} \cdot \text{cm}^{-2} \cdot \text{sec}^{-1}$$

$$N_{G,beg} = (3.26 \pm 0.05) \text{ pulse} \cdot \text{cm}^{-2} \cdot \text{sec}^{-1}$$

Subtracting the background, we obtain the counter readings resulting from the radiation that causes the high intensity. From column 8, Table 1, it follows that the mean value of the ratio of registration of this radiation by the Geiger and scintillation counters is

$$\frac{N_G - N_{G,beg}}{N_{sc} - N_{sc,beg}} = \frac{\epsilon_G}{\epsilon_{sc}} \approx 3 \cdot 10^{-3}$$

Consequently, the given radiation is  $\gamma$  radiation with an energy of the order of 100-300 kev. The mean energy of secondary electrons, appearing in the crystal due to bremsstrahlung, may be estimated according to the data of column 7; it is of the order of 10<sup>5</sup> ev.

In Table 2 is a series of counter readings during flight through the zone of increased intensity in the Southern hemisphere. The cosmic background deduction was made in a similar fashion. Counter readings obtained in the  $+70$  to  $+180^\circ$  longitude range during the flight through the zone of increased intensity were used for that purpose. The mean value of the cosmic background in the Southern hemisphere was found to be

$$N_{sc,beg} = (12.0 \pm 0.4) \text{ pulse} \cdot \text{cm}^{-2} \cdot \text{sec}^{-1}$$

$$E_{beg} = (3.27 \pm 0.07) 10^7 \text{ ev} \cdot \text{cm}^{-2} \cdot \text{sec}^{-1}$$

$$N_{G,beg} = (3.08 \pm 0.05) \text{ pulse} \cdot \text{cm}^{-2} \cdot \text{sec}^{-1}$$

It follows also from Table 2 that the increased intensity is due to bremsstrahlung electrons with energy near 200 kev, thus about the same as for the Northern hemisphere.

Therefore, the point-by-point relationship (by magnetic lines of force) between the zones of increased intensity in the Northern and Southern hemispheres, the coincidence of the geographic position of the zones with the mirror point lines for particles captured by the earth's magnetic field and the well-defined nature of the registered radiation and its energy indicate that the recorded increased intensity is due to electrons of the outer radiation belt, decelerated by the skin of the spaceship satellite.

As stated, a lower intensity is being observed in separate observation zones, at points with greater magnetic field intensity. However, no net connection between the intensity of radiation and that of the magnetic field is generally indicated when going over the map. This is apparently because electrons of the outer radiation belt are short-lived, especially at examined heights in comparison with the drift time around the earth. Assuming that at 300 km altitude the density of the atmosphere is  $3.5 \cdot 10^9 \text{ atom} \cdot \text{cm}^{-3}$ , we calculate for electrons with energies of 10<sup>5</sup> ev at that height, a lifetime of the order of several seconds (5). This is much less than the drift time around the earth for electrons with the same energies. Therefore, electrons perish in the atmosphere after a comparatively small number of oscillations from one hemisphere to the other, and they have no time to shift significantly by longitude.

Knowing the number of oscillations, the electron flux at 300 km (which, according to measurements on the second spaceship satellite, has a  $5 \cdot 10^4$  electron  $\cdot$  cm $^2$   $\cdot$  sec $^{-1}$  intensity), and the width of the radiation belt at that altitude around the earth, one may determine the lower limit of the total electron outflow from the outer belt and, consequently, estimate the upper limit of electron lifetime in the belt.

The estimates carried out give electrons with energies of 300 kev at  $10^6$ – $10^8$  sec lifetime and show that between the two hypotheses of the origin of energetic electrons in the outer radiation belt, the hypothesis of the local electron acceleration within the limits of the geomagnetic field seems to be rather more valid than that of the neutron decay.

### Reviewer's Comment

The first part of this paper is an extension of the descriptions of the lower edge of the Van Allen belt that have been made by Yoshida et al. (1) and others. In light of the results of the Argus experiment, which tied together magnetic conjugate points with trapped radiation (2), the results discussed in the first part of this paper may be considered as confirmation of previous descriptions of the radiation belt—for example, see Chap. 3 of the *Satellite Environment Handbook* (3).

The most significant feature of this paper is the method suggested by the authors of estimating the electron lifetime based on loss-rate measurements. Essentially the same method has been employed by Hess, Bloom, Mann, Seward, and West (4) in an independent approach to the outer zone electron lifetime problem. This work, using Discoverer satellites orbiting at essentially the same altitude as the Mechta flights, comes to strikingly different conclusions from those of Vernov et al. Hess and co-workers are able to identify two distinct groups of outer zone electron particles: a) a low energy group ( $E < 200$  kev) which has a short lifetime and shows rapid time variations in intensity, and b) a high energy group ( $E > 200$  kev) which is very stable in time and appears to be lost only over the South Atlantic (i.e., Capetown) anomaly. The lifetime of the low energy group has been estimated by O'Brien (5) to be less than about  $10^5$  sec, whereas Hess et al. estimate the lifetime of the high energy component to have a lifetime of the order of  $10^{10}$  sec.

Since Vernov et al. have not differentiated between these two different electron populations, their electron lifetime

The authors are grateful to A. E. Chudakov, I. P. Ivanenko, and E. V. Gorchakov for the discussion of the results obtained.

—Submitted May 23, 1961

### References

- 1 Vernov, S. N. and Chudakov, A. E., *Trudy Mezhdunar. Kom. Kosmich. Lucham* (Transactions of the International Conference on Cosmic Rays) (Publishing House of the Academy of Science USSR), no. III, 17 (1960).
- 2 "The second Soviet spaceship," *Izdatel'stvo Pravda* (Publishing House, Pravda) (1960).
- 3 Vestine, E. H. and Sibley, W. L., *Planetary Space Sci.* **1**, 285 (1959).
- 4 Cladis, J. B. and Dessler, A. J., *J. Geophys. Res.* **66**, 343 (1961).
- 5 Welsh, J. A. and Whitaker, W. A., *J. Geophys. Res.* **64**, 909 (1959).

estimate of  $10^6$ – $10^8$  sec might represent some average between the lifetimes calculated by O'Brien and by Hess et al.

The method used by both Vernov et al. and Hess et al. to calculate electron lifetime uses the concept of a mirror point drift velocity which has been criticized as invalid. It is generally acknowledged that the rigorously correct method of performing the loss-rate calculation is to solve the time-dependent Foker-Planck equation as discussed by Walt and MacDonald (6), and Wentworth, MacDonald, and Singer (7).

In spite of these uncertainties, the final conclusion reached by Vernov and co-workers, i.e., that the outer zone electrons seem to be due to an as yet unknown local acceleration process rather than the neutron decay, appears valid. Even if neutron decay acts as an injection source, the various measurements make it clear that in all energy ranges (and in particular at low energies) a particle acceleration mechanism is acting within the geomagnetic field.

—A. J. DESSLER  
Southwest Center for  
Advanced Studies

- 1 Yoshida, S., Ludwig, G. H., and Van Allen, J. A., *J. Geophys. Res.* **65**, 807 (1960).
- 2 Van Allen, J. A., McIlwain, C. E., and Ludwig, G. H., *J. Geophys. Res.* **64**, 877 (1959).
- 3 *Satellite Environment Handbook*, edited by F. S. Johnson (Stanford University Press, 1961).
- 4 Hess, W. N., Bloom, S., Mann, L., Seward, F., and West, M., "Electron loss rate from the outer radiation belt," presented at Third International Space Sciences Symposium, COSPAR, Washington, D. C. (May 1962).
- 5 O'Brien, B. J., *J. Geophys. Res.* **67**, 1227 (1962).
- 6 MacDonald, W. M. and Walt, M., *Ann. Phys.* **15**, 44 (1961).
- 7 Wentworth, R. C., MacDonald, W. M., and Singer, S. F., *Phys. Fluids* **2**, 499 (1959).